Progress In Electromagnetics Research M, Vol. 65, 51–60, 2018

Multi-Band Fractaled Triangular Microstrip Antenna for Wireless Applications

Mohd G. Siddiqui*, Abhishek K. Saroj, Devesh, and Jamshed A. Ansari

Abstract—The proposed microstrip antenna is based on fractal techniques and designed for wireless applications. The radiating element is an A-shaped triangle on which fractal concept is applied. Fractal concept is applied on the proposed A-Shaped Fractal Microstrip Antenna (ASFM-Antenna), similar to English alphabet letter A. Further the analysis and verification of result is achieved by testing the fabricated antenna and also comparison of simulated and experimental results. Von Koch's snowflake concept is used in which a single line is divided into four new lines, and it is done at each side of the triangle. This step is repeated. In this paper, a two-iteration Koch generator is used, thus the proposed antenna is designed. Simulations are carried out using commercially available HFSS (High Frequency Structure Simulator) based on finite element method. The antenna is simulated and fabricated, and results are recorded. It is found that simulated and experimental results are in close agreement with each other. The antenna resonates at 11.44 GHz, 13.178 GHz, 15.482 GHz, 19.902 GHz and 23.529 GHz. Hence, X-band [8.2–12.4 GHz], Ku-band [12.4–18 GHz] and K-band [18–26.5 GHz] are the frequencies of operating bands under consideration.

1. INTRODUCTION

The combination of fractal geometry with microstrip patch antenna design has led to the development of fractal antennas. Fractal geometries as described by Mandelbrot [1] are uneven shapes which can be separated into sub-parts, and every sub-part is a small copy of the overall shape. The fractal shape acts as a radiating element of copper or gold metal which is etched on a dielectric substrate. Fractal antenna application in engineering is firstly discussed by Cohen in [2]. This type of antenna geometry is useful for military, satellite and wireless applications.

A numbers of fractal geometries are presented in the literature such as Sierpinski's gasket, Von Koch's snowflake, Sierpinski-Koch and Koch-Sierpinksi shapes. A Koch-like fractal curve is designed by Li and Mao [3] to transform an ultra-wideband (UWB) bow-tie into a so called Koch-like sided fractal bow-tie dipole. The behavior of the small fractal Koch monopole is numerically and experimentally analyzed by Baliarda et al. [4]. The main advantage of using fractal geometry as the radiating element is its more electrical length fitting into small areas. Werner et al. in [5] explained frequency independent features of self-similar fractal antennas. Usually, fractal antennas using fractal geometries are used for miniaturization [6], space-filling and multiband application [7, 8]. The design of a Pythagorean tree fractal patch antenna is done by Silva et al. [9], where squares are made on the base of the radiating patch. The antenna is designed to achieve multiband characteristics. Also, a Pythagorean-shaped iterated fractal antenna is realized in [10] by Kumar et al. The multiband fractal antenna design of Pythagoras tree shapes is previously done by Kumar et al. [11]. A novel Koch Snowflake and Sierpinski Carpet combined fractal multiband antenna is proposed by Yu et al. [12] for 2G/3G/4G/5G/WLAN/Navigation wireless applications, based on principles of conventional microstrip monopole antenna and resonant

Received 10 January 2017, Accepted 10 February 2018, Scheduled 26 February 2018
* Corresponding author: Mohd Gulman Siddiqui (mohdgulman@gmail.com).
The authors are with the Department of Electronics and Communication, University of Allahabad, Allahabad, UP, India.

coupling technique, combined with advantages of fractal geometry. Also, a fractal by Eskandari et al. [13], in arms of an antipodal dipole for antenna miniaturization, uses the Chu's sphere very effectively to keep antenna efficiency very high. Complex plane fractal Mandelbrot set geometries, which are of the escape-time fractal type, are used in the development of microstrip patch antennas fed by a coaxial cable. These antennas are developed for near millimeter-wave application done by Minervino et al. in [14]. The fractal concept increases the electrical size of the antenna by increasing perimeter of the geometry no matter square, circle or triangle. Thus miniaturization is done by this methodology [15, 16].

In this paper, A-shape of MSA is designed and analyzed based on Koch Snowflake fractal geometry. Koch generator is applied at each edge of the radiating element. After two iterations, multiband operation is obtained in the proposed antenna. The antenna covers frequency range useful for wireless applications which are 11.44 GHz, 13.178 GHz, 15.482 GHz, 19.902 GHz and 23.529 GHz. The design of antenna is done using FEM based simulator Ansoft designer HFSS. The following sections include antenna design and its configurations, Koch fractal concept technique and its implementation, and discussion of results.

2. ANTENNA DESIGN AND ITS EQUIVALENT CIRCUIT

The fabricated geometry of the proposed ASFM-Antenna for top view, side view and back view is shown in Fig. 1. The geometry is excited by a coaxial probe of 50 ohm input impedance at the feed point location of (0, 9.35), and it is loaded with number of notches. The antenna consists of an A-shape isosceles triangle with two equal sides as 60 mm and a larger base as 70 mm. The suggested antenna is assembled on an FR4 substrate with dielectric constant (ε_r)4.4. In the proposed antenna design, FR4 glass epoxy dielectric material of height (h) 1.6 mm has dimension $80 \times 90\,\text{mm}^2$. Microstrip antenna can be considered equivalent to an R-L-C parallel circuit. The equivalent circuit of proposed antenna is changed according to slots, notches and other techniques involved in the design for improvement or enhancement purpose. Through it we can calculate the resonant frequency of the design. The proposed antenna is considered as a parallel combination of resistance (R_1), inductance (L_1), and capacitance (C_1) as shown in its equivalent circuit of Fig. 2 and can be given as,

$$C_1 = \frac{LW\varepsilon_0\varepsilon_e}{2L}\cos^2(\pi Y_0/L) \tag{1}$$

$$R_1 = Q/\omega_r^2 C_1 \tag{2}$$

$$L_1 = 1/\omega_r^2 C_1 \tag{3}$$

A-shaped triangle radiating patch is used here with 60 mm of equal sides and a 70 mm base. The feed point location is an important parameter on which many constraints depend. The dimensions are shown in Table 1. Here, all dimensions are marked such as length of sides of triangle, height of substrate, dielectric constant, feed point location and both the axes of 2-D plane. After performing

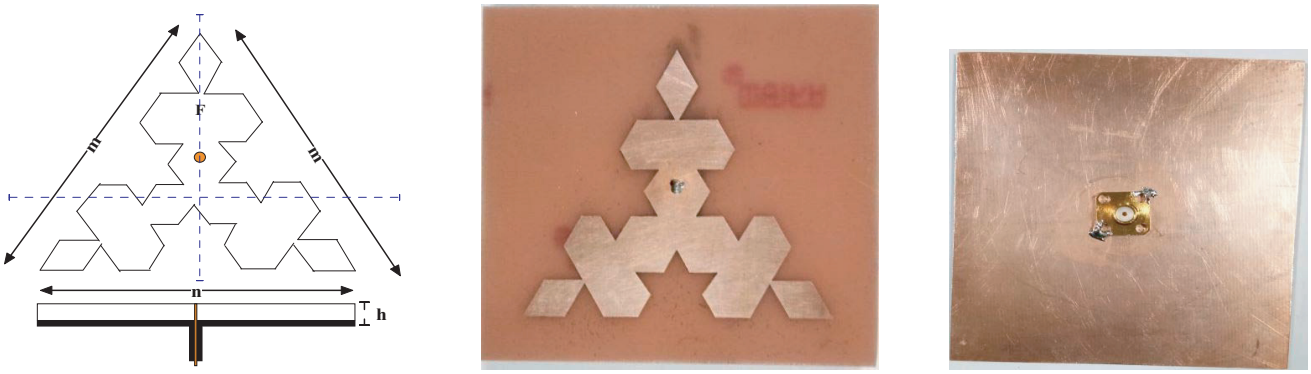

(a) (b) (c)

Figure 1. (a) Geometry of ASFM-Antenna, top and side view. (b) Fabricated design top view, and (c) fabricated design bottom view with co-axial feeding.

Table 1. Dimensions of proposed antenna.

Length of perpendicular height of triangle **(m)**	60 mm
Length of the base of triangle **(n)**	70 mm
Location of Feed Point **(F)**	(0, 9.35)
Dielectric constant (ε_r)	4.4
Thickness of Substrate **(h)**	1.57 mm

Table 2. Comparison of proposed antenna with conventional antenna.

S. No.	**Parameters**		
		Conventional triangular Antenna*	**ASFM-Antenna**
1	Area	2121.7622 mm^2	1430 mm^2
2	% Reduction	-	32.602%
3	Electrical Length	Perimeter of triangle	Widely increased
4	Bands	Single or double band [**21, 22**]	Multiband
5	Frequency band	S, C-Bands etc.	K, Ku-band

* considering that the size of conventional antenna assumes the same size of triangle as for ASFM-Antenna.

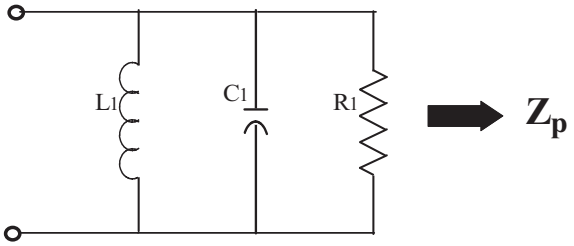

Figure 2. Equivalent circuit of patch disk.

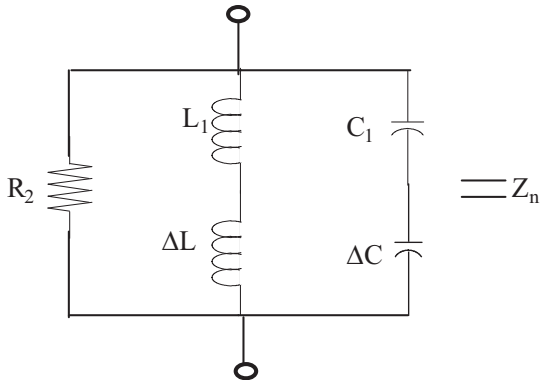

Figure 3. Equivalent circuit of notch.

several simulations, results are analyzed and saved. Table 2 shows comparison of the proposed ASFM-Antenna with a conventional antenna.

The equivalent circuit of a slot comprises a series combination of radiation resistance and reactive components. Loading a notch incurs a parallel combination of resistance, inductance and capacitance. So the overall analysis of the design is changed. Ansari et al. [17, 18] show the equivalent circuit of slots and notches loaded in a microstrip antenna.

Here, L is the length of rectangular patch, W the width of rectangular patch, Y_o the feed point location, h the thickness of substrate material, c the velocity of light, f the design frequency, and ε_o the effective permittivity of the medium.

$$\varepsilon_e = \frac{\varepsilon_r + 1}{2} + \frac{\varepsilon_r - 1}{2}\left[1 + \frac{12h}{W}\right]^{-1/2} \tag{4}$$

ε_e is the relative permittivity of substrate, and $Q = \frac{c\sqrt{\varepsilon}_o}{4fh}$ is the quality factor.

$$Z_p = \frac{1}{\dfrac{1}{R_1} + j\omega C_1 + \dfrac{1}{j\omega L_1}} \tag{5}$$

Z_p is the impedance of rectangular patch. In this rectangular patch, a number of notches are loaded. A single notch causes the flow of two currents in the patch. One is normal patch current that causes the antenna to resonate at the design frequency of initial patch, and the other current flows around the notch which results in another resonant frequency.

Due to notch an additional series inductance (ΔL) and series capacitance (ΔC) modify the equivalent circuit of antenna. This can be seen in Fig. 3.

$$L_1 = L + \Delta L, \quad \text{and}$$
$$C_1 = \frac{C\Delta C}{C + C\Delta C}$$

The rectangular patch and notch-loaded patch are coupled through mutual inductance (L_m) and mutual capacitance (C_m).

$$\Delta L = \frac{H\eta\pi}{8}(L_n/W_n), \tag{6}$$

$$\Delta C = \left(\frac{L_n}{W_n}\right) C_g \tag{7}$$

where $\mu = 4\pi \times 10^{-7}$ H/m, C_g = gap capacitance.

The impedance of notch loaded on the substrate as shown in Fig. 4 can be given as,

$$Z_n = \frac{1}{\frac{1}{R_2} + j\omega C_2 + \frac{1}{j\omega L_2}}, \tag{8}$$

The value of R_2 resistance after cutting the notch is calculated, in which L_m and C_m are mutual inductance and capacitance between the two resonators. The notch-loaded patch can be shown as in Fig. 4.

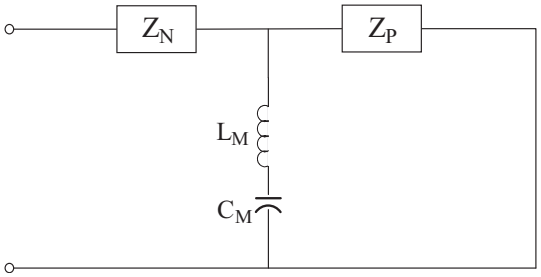

Figure 4. Equivalent circuit of coupled notch-loaded patch antenna.

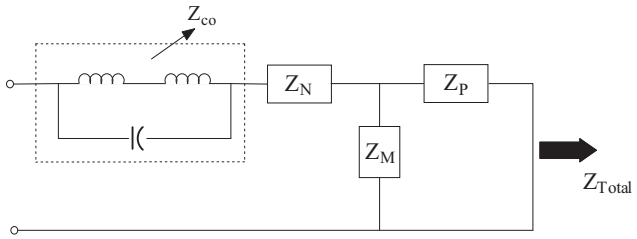

Figure 5. Equivalent circuit of co-axial feed notch-loaded patch antenna.

The proposed ASFM-Antenna after inserting a number of fractal notches using coaxial feed can be shown as in Fig. 5.

Here, Z_{co} is the impedance of co-axial feed.

$$\mathbf{Z_{Total}} = \frac{\mathbf{Z_m + Z_p}}{\mathbf{Z_m Z_p}} + \mathbf{Z_N} + \mathbf{Z_{CO}} \tag{9}$$

Now using $\mathbf{Z_{Total}}$, the calculation of total input impedance and various parameters such as reflection co-efficient, VSWR and return loss can be done.

$$\text{Reflection co-efficient,} \quad \Gamma = \frac{\mathbf{Z_{Total} - Z}}{\mathbf{Z_{Total} + Z}} \tag{10}$$

$$\text{Return Loss,} \quad RL = 20\log|\Gamma| \tag{11}$$

$$\text{VSWR} = \frac{1+\Gamma}{1-\Gamma} \tag{12}$$

$$\text{Bandwidth,} \quad BW = \frac{2(f_h - f_l)}{(f_h - f_l)} \times 100\% \tag{13}$$

3. KOCH FRACTAL CONCEPT

The proposed isosceles triangle is based on Von Koch's snowflake. The design of fractal geometry is done using Koch curve concept. Koch curve concept is based on generating L Euclidian segment which is divided into three segments. The method of dividing the line segment and number of iterations is shown in Fig. 6. Here it is clear that a line segment is divided into three parts, and the middle section is replaced by an equilateral triangle with base line removed. This method of iteration Koch curve is applied on the proposed isosceles triangle at each side of the isosceles triangle.

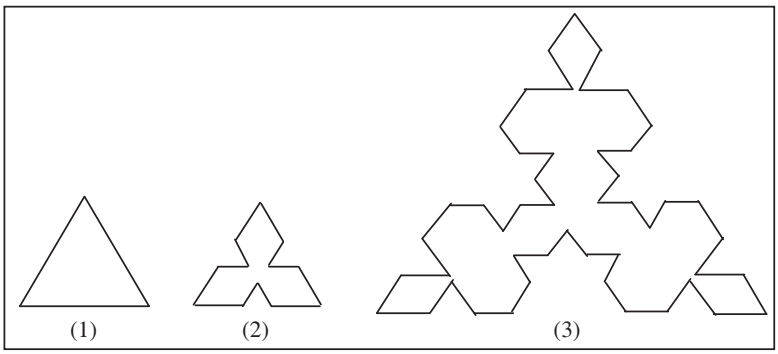

Figure 6. Process of designing proposed antenna using Koch generator.

After each iteration, the length of each line is increased to 4th/3rd to the original. The new length becomes L_n as in Equation (1).

$$L_n = L(4/3)^n \tag{14}$$

Here L is the length of the original line, L_n the length of the new line after (n) iteration, and (n) the number of iterations. In the proposed isosceles triangle, number of iterations is $n = 2$.

The Koch snowflake is constructed by adding smaller and smaller triangles to the structure in an iterative fashion. The first three stages in the construction of the standard Koch curve are via an IFS (Iterative Function System) approach. The transformation is applied for each iteration to achieve higher levels of fractalization.

These iterated function systems are based on the application of a series of affine transformations, w, defined by

$$w\begin{pmatrix} x \\ y \end{pmatrix} = \begin{pmatrix} a & b \\ c & d \end{pmatrix}\begin{pmatrix} x \\ y \end{pmatrix} + \begin{pmatrix} e \\ y \end{pmatrix} \tag{15}$$

$$\text{or,} \quad w(x, y) = (ax + by + e, cx + dy + f) \tag{16}$$

a, b, c, d, e and f are real numbers. Hence affine transformation, w, is replaced by six parameters,

$$\left(\begin{array}{cc|c} a & b & e \\ c & d & f \end{array}\right), \tag{17}$$

Here a, b, c and d are control rotation and scaling, while e and f are control linear translation.

Now suppose that we consider w_1, $w_2, \ldots, w_N$ as a set of affine linear transformations, and let A be the initial geometry, produced by applying the set of transformations to the original geometry, A, and collecting the results from $w_1(A)$, $w_2(A), \ldots, w_N(A)$, which can be represented by,

$$w(A) = \bigcup_{n=1}^{N} w_N(A), \tag{18}$$

Here w is known as Hutchinson operator. A fractal geometry can be obtained by repeatedly applying w to the previous geometry.

For e.g., if the set A_0 represents the initial geometry, then we will have,

$$A_1 = w(A_0), \quad A_2 = w(A_1) \ldots A_{k+1} = w(A_k) \tag{19}$$

An iterated function system generates a sequence that converges to a final image,

$$w(A_\infty) = A_\infty \tag{20}$$

This image is called the attractor of the iterated function system, and represents a "fixed point" of w [19].

Here,

$$W(x) = \begin{bmatrix} a & b \\ c & d \end{bmatrix} \begin{pmatrix} x_1 \\ x_2 \end{pmatrix} + \begin{pmatrix} e \\ f \end{pmatrix}$$

$$a = \frac{1}{s}\cos\theta, \quad b = -\frac{1}{s}\sin\theta, \quad c = \frac{1}{s}\sin\theta, \quad d = \frac{1}{s}\cos\theta$$

Therefore, with the help of Iterated Function System (IFS), the proposed ASFM-Antenna is designed.

The values of scale factors s and θ are 1/3 and 60°, respectively. Hence the matrix can be filled for the proposed antenna parameters. Table 3 and Table 4 correspond to the value of similarity transformation which is calculated with the help of Fig. 7, and it is referred from [20].

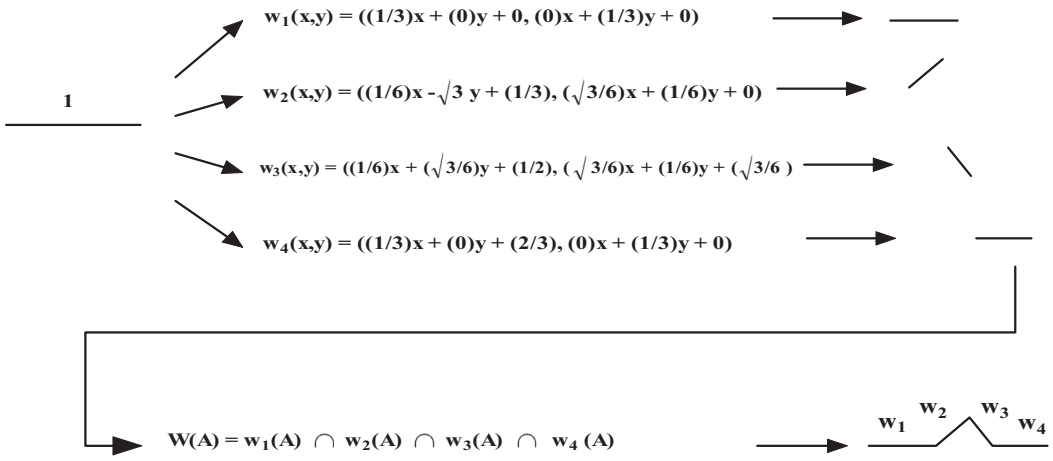

Figure 7. The standard Koch curve as iterated function system (IFS).

Table 3. Similarity transformation of Koch collage.

NUMBER K	SCALE S	ROTATION Θ	TRANSLATION T_X	T_Y
1	1/3	0°	0	0
2	1/3	60°	1/3	0
3	1/3	−60°	1/2	$\sqrt{3}/6$
4	1/3	0°	2/3	0

Table 4. Formulas for similarity transformation of Koch curve collage.

TRANSFORMATION	X-PART	Y-PART
$w_1(x,y)$	$(1/3)x$	$(1/3)y$
$w_2(x,y)$	$(1/6)x - (\sqrt{3}/6)$y+(1/3)	$(\sqrt{3}/6)x + (1/6)y$
$w_3(x,y)$	$(1/6)x + (\sqrt{3}/6)y + (1/2)$	$-(\sqrt{3}/6)x + (1/6)y + (\sqrt{3}/6)$
$w_4(x,y)$	$(1/3)x + (2/3)$	$(1/3)y$

$$\text{So,} \quad \begin{bmatrix} a & b \\ c & d \end{bmatrix} = \begin{bmatrix} 1/3 & 0 \\ 0 & 1/3 \end{bmatrix} \quad \text{for} \quad \theta = 0^\circ,$$
$$= \begin{bmatrix} 1/6 & -\sqrt{3}/6 \\ \sqrt{3}/6 & 1/6 \end{bmatrix} \quad \text{for} \quad \theta = 60^\circ,$$
$$= \begin{bmatrix} 1/6 & \sqrt{3}/6 \\ -\sqrt{3/6} & 1/6 \end{bmatrix} \quad \text{for} \quad \theta = -60^\circ,$$
$$= \begin{bmatrix} 1/3 & 0 \\ 0 & 1/3 \end{bmatrix} \quad \text{for} \quad \theta = 0^\circ,$$

4. DISCUSSION OF RESULTS

The simulation of proposed ASFM Antenna is done by ANSOFT HFSS software. The multiband response is recorded after performing the simulation, and number of minima is achieved. The fractal antenna generally gives multiband characteristics.

The results obtained by simulation software are verified by testing of the fabricated antenna using VNA (vector network analyzer). The results are seen in agreement with each other, and it is said to be a good design for particular applications.

Figure 8 shows the return loss versus frequency of the proposed antenna. Simulated and measured plots are compared here. It is seen that multiband resonance is achieved in the plots. Further, it is observed that bands of simulated and measured results are approximately matched with some variations particularly at higher resonance. This variance is due to human error occurring in fabrication and testing process. Simulations are based on ideal boundary conditions while measured result incurs several losses as well.

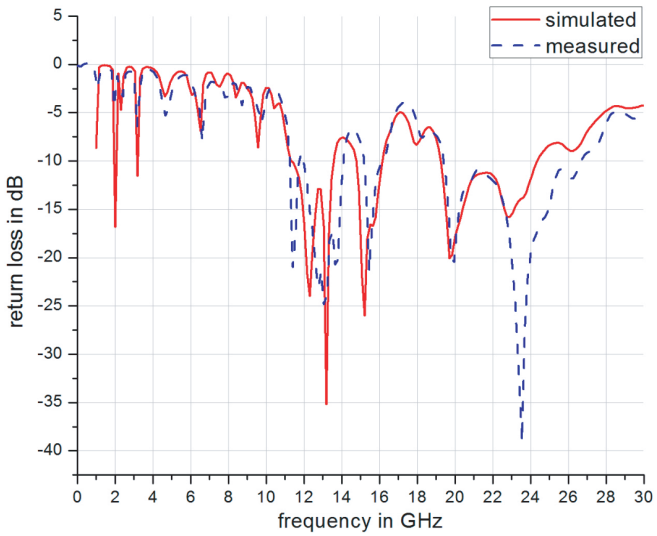

Figure 8. Plot of return loss versus frequency of simulated and experimental result of proposed ASFM-Antenna.

It is seen that the antenna resonates at 12.31 GHz, 13.18 GHz, 15.21 GHz and 19.7 GHz covering the operating frequency band of Ku-band [12–18 GHz] and K-band [18–27 GHz]. Hence these bands show that the antenna is capable of using for commercial purpose and for satellite applications as well.

Figure 9 shows the snapshot of experimental result through VNA. The return loss versus frequency plot is recorded at frequencies 11.44 GHz, 13.178 GHz, 15.482 GHz, 19.902 GHz and 23.529 GHz with return losses of −19 dB, −27.37 dB, −20.16 dB, −20.74 dB and −35.52 dB, respectively.

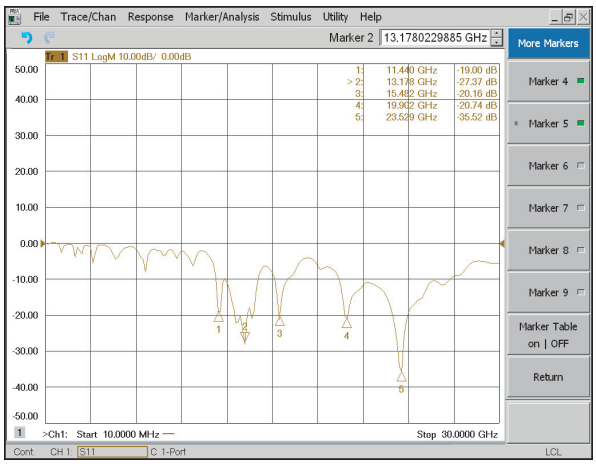

Figure 9. Experimental result of return loss versus frequency of proposed ASFM-Antenna using VNA (vector network analyzer).

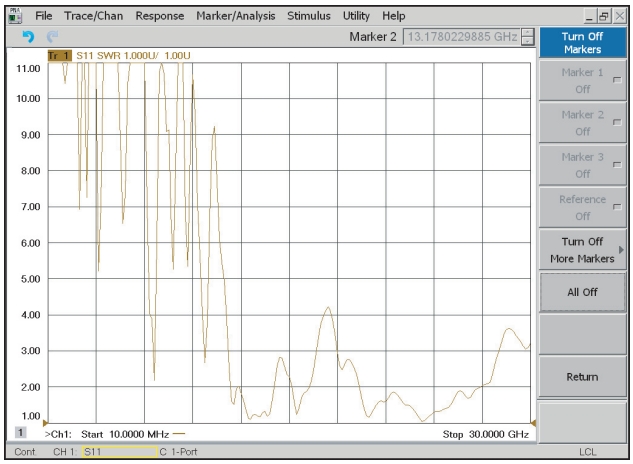

Figure 10. Experimental result of VSWR versus frequency of proposed ASFM-Antenna using VNA (Vector Network Analyzer).

Figure 11. Radiation pattern measurement of proposed ASFM-Antenna using anechoic chamber.

Figure 10 shows a snapshot of measured reflection coefficient with frequency using VNA. It is clear that at each resonant frequency the value of VSWR is well between 1 and 2. So, the proposed antenna has good matching between transmitter and receiver.

Figure 11 shows the radiation pattern measurement using an anechoic chamber. The fabricated ASFM-Antenna is mounted on top of the mount, while the receiving horn antenna at the other end. The setup is excited first using coaxial cable and is observed under a lossless anechoic chamber as seen in Fig. 11. The results are recorded from angle 0° through 360° rotation and saved.

Fig. 12 shows the radiation pattern at lower (12.31 GHz) frequency then 13.18 GHz, 15.21 GHz, respectively. The simulated resonant frequency is in approximation with measured one. The E-plane and H-plane for each resonant frequency can be seen.

Figure 13 shows the measured E/H-plane radiation pattern from lower 11.44 GHz, 13.178 GHz and higher 15.482 GHz frequencies. In both Fig. 12 and Fig. 13, the radiation pattern is shown only at three resonant frequencies.

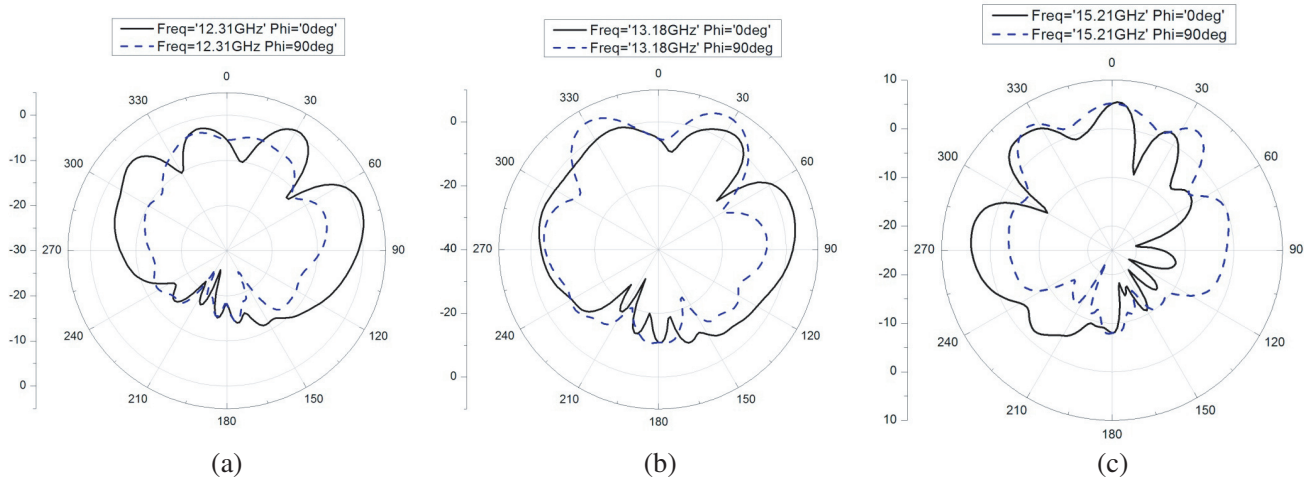

Figure 12. Simulated E/H-plane radiation pattern at (a) 12.31 GHz, (b) 13.18 GHz, and (c) 15.21 GHz of ASFM-Antenna.

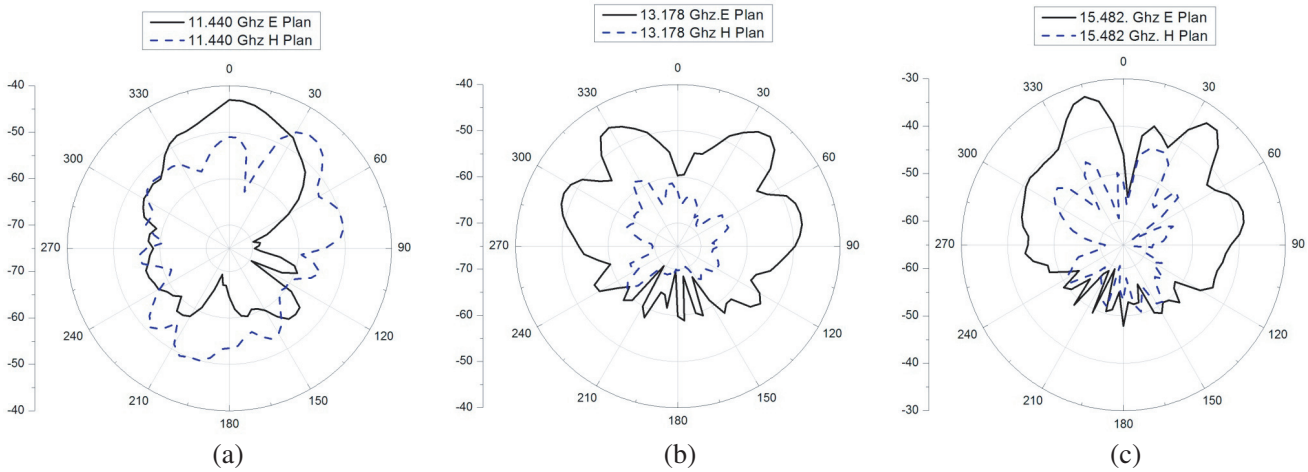

Figure 13. Measured E/H-plane radiation pattern at (a) 11.44 GHz, (b) 13.178 GHz, and (c) 15.482 GHz of ASFM-Antenna.

5. CONCLUSION

In this work, a Koch-fractal based microstrip antenna for multiband operation is designed. The analysis of the coaxial feed antenna is theoretically analyzed using cavity model method, and the proposed antenna is simulated using Ansoft Designer. Then it is tested, and results obtained are found in agreement with each other. The paper also suggests that the size of antenna is reduced as compared to a conventional antenna. Also a multiband resonance is seen at higher frequency. The proposed antenna exhibits frequency operation at 11.44 GHz, 13.178 GHz, 19.902 GHz and 23.529 GHz with sufficient return loss. This antenna can be useful for X-band, Ku-band and K-band applications.

REFERENCES

1. Mandelbrot, B. B., *The Fractal Geometry of Nature*, W. H. Freeman, New York, 1983.
2. Cohen, N., "Fractal antenna application in wireless telecommunication," *Proceeding of Electronics Industries Forum of New England*, 43–49, 1997.

3. Li, D. and J.-F. Mao, "A Koch-like sided fractal bow-tie dipole antenna," *IEEE Transactions on Antennas and Propagation*, Vol. 60, No. 5, 2242–2251, May 2012.
4. Baliarda, C. P., J. Romeu, and A. Cardama, "The Koch monopole: A small fractal antenna," *IEEE Transactions on Antennas and Propagation*, Vol. 48, No. 11, 1773–1781, Nov. 2000.
5. Werner, D. H., P. L. Werner, and A. J. Ferraro, "Frequency independent features of self-similar fractal antennas," *Antennas Propag. Soc. Int. Symp., AP-S. Dig.*, Vol. 3, 2050–2053, Jul. 1996.
6. Gianvittorrio, J. P. and Y. Rahmat-Samii, "Fractal antennas: A novel antenna miniaturization technique and applications," *IEEE Antennas and Propagation Magazine*, Vol. 44, 20–36, 2002.
7. Viani, F., M. Salucci, F. Robol, and A. Massa, "Multiband fractal ZigBee/WLAN antenna for ubiquitous wireless environments," *Journal of Electromagnetic Waves and Applications*, Vol. 26, No. 11-12, 1554–1562, Aug. 2012.
8. Puente, C., J. Romeu, R. Pous, and A. Cardama, "On the behavior of the Sierpinski multiband fractal antenna," *IEEE Transactions on Antennas and Propagation*, Vol. 46, No. 4, 517–524, Apr. 1998.
9. Silva, H. A. M., A. G. D'Assunção, and J. P. Silva, "Design of modified pythagorean fractal antenna for multiband application," *2017 International Applied Computational Electromagnetics Society Symposium — Italy (ACES)*, 1–2, Florence, 2017.
10. Kumar, A., B. R. Dutta, and S. Budhauliya, "Iterated Pythagorean fractal tree multiband antenna," *Int. Journal Scientific Res. Pub.*, Vol. 3, No. 9, 1–3, 2013.
11. Kumar, D., A. Kumar, and A. K. Singh, "Design analysis of Pythagoras tree shaped multiband fractal antenna," *Int. Conf. Comput. Intelligence Commun. Networks (CICN)*, Bhopal, 41–45, 2014.
12. Yu, Z., J. Yu, X. Ran, and C. Zhu, "A novel Koch and Sierpinski combined fractal antenna for 2G/3G/4G/5G/WLAN/navigation applications," *Microwave and Optical Technology Letters*, Vol. 59, 2147–2155, 2017.
13. Eskandari, Z., J. Ahmadi-Shokoh, A. Keshtkar, and L. Ghanbari, "A novel fractal for improving efficiency and its application in LTE mobile antennas," *Microwave and Optical Technology Letters*, Vol. 57, No. 10, Oct. 2015.
14. Minervino, D. R., A. G. D'Assuncao, and C. Peixeiro, "Mandelbrot fractal microstrip antennas," *Microwave and Optical Technology Letters*, Vol. 58, No. 1, Jan. 2016.
15. Oliveira, E. E. C., P. H. F. Silva, A. L. P. S. Campos, and A. G. D'Assuncao, "Small-size quasi-fractal patch antenna using the Minkowski curve," *Microwave and Optical Technology Letters*, Vol. 52, 805–809, 2010.
16. Silva, M. R., C. L. N. obrega, P. H. F. Silva, and A. G. D'Assuncao, "Optimal design of frequency selective surfaces with fractal motifs," *IET Microwaves Antennas Propag.*, Vol. 8, 627–631, 2014.
17. Ansari, J. A., N. P. Yadav, P. Singh, and A. Mishra, "Compact half U-slot loaded shorted rectangular patch antenna for broadband operation," *Progress In Electromagnetics Research M*, Vol. 9, 215–226, 2009.
18. Ansari, J. A., A. Mishra, N. P. Yadav, P. Singh, and B. R. Vishvakarma, "Compact triple U-shaped slot loaded circular disk patch antenna for bluetooth and WLAN application," *International Journal of Microwave and Optical Technology*, Vol. 6, No. 2, Mar. 2011.
19. Werner, D. H. and S. Ganguly, "An overview of fractal antenna engineering research," *IEEE Antennas and Propagation Magazine*, Vol. 45, No. I, Feb. 2003.
20. Peitgen, H. O., H. Jurgens, and D. Saupe, *Chaos and Fractals New Frontiers of Science*, Springer-Verlag, Inc., New York, 1992.
21. Wong, K.-L. and S.-C. Pan, "Compact triangular microstrip antenna," *Electronics Letters*, Vol. 33, No. 6, 433–434, Mar. 13, 1997.
22. Vishwakarma, R. K., J. A. Ansari, and M. K. Meshram, "Equilateral triangular microstrip antenna for circular polarization dual-band operation," *Indian Journal of Radio & Space Physics*, Vol. 35, 293–296, Aug. 2006.